

# Measurement of Moisture Storage Parameters of Building Materials

M. Jiříčková, R. Černý, P. Rovnaníková

*The moisture storage parameters of three different building materials: calcium silicate, ceramic brick and autoclaved aerated concrete, are determined in the hygroscopic range and overhygroscopic range. Measured sorption isotherms and moisture retention curves are then combined into moisture storage functions using the Kelvin equation. A comparison of measured results with global characteristics of the pore space obtained by mercury intrusion porosimetry shows a reasonable agreement; the median pore radii by volume are well within the interval given by the beginning and the end of the characteristic steep parts of the moisture retention curves.*

*Keywords: moisture retention curve, sorption isotherm, desorption isotherm, building materials.*

## 1 Introduction

Application of mathematical and computational models to simulate transport processes in building materials requires knowledge of the material parameters that are used as input parameters of the models. Two basic types of such parameters can be recognized, i.e., transport parameters and storage parameters.

Transport parameters are the phenomenological coefficients that appear in the constitutive equations as proportionality factors between the generalized thermodynamic forces and fluxes.

Storage parameters need to be defined because transport equations are generally formulated for particular mass and energy densities, and in their original form they do not contain the basic state variables that appear (in the form of their gradients) in the constitutive equations. The main role of storage parameters is that they make it possible to calculate the partial derivatives of the particular mass or energy densities with respect to the basic state variables.

In modeling moisture transport, it is necessary to include in the transport equation at least one moisture storage parameter, depending on the class of moisture transport model. However, it is physically more correct to define two parameters, one for the hygroscopic range, and the second for the overhygroscopic range. In the hygroscopic range, the sorption (or desorption) isotherm is the main parameter used in most models, while in the overhygroscopic range, the moisture retention curve is employed. These two moisture storage parameters can be combined in a single relation, the moisture storage function, using the Kelvin equation (see, e.g., [1] for more details).

The sorption and desorption isotherms of porous building materials are very frequently measured in building-physics laboratories, and extensive catalogues are available for many materials (e.g., [2]). On the other hand, measurements of moisture retention curves for building materials are still relatively rare (e.g., [3], [4]), in contrast to the numerous measurements on soils (see, e.g., [5] for an overview). The main reason for this is that building physicists have until now seen more interested in knowing the moisture related properties in the hygroscopic range than in the overhygroscopic range. This attitude is also reflected in most building

physical standards all over the world, where liquid water related properties are not considered.

The neglect of liquid water transport and storage properties in calculations related to building physics may lead in many cases to a significant departure from reality. Typical examples are situations where wind driven rain plays an important role, where there is rising damp in a building, or when capillary active or hydrophilic interior thermal insulation is used. Therefore, simultaneous utilization of both liquid water and water vapor related transport and storage properties in computational codes is very desirable, and advanced codes already take them into account (e.g., [6]).

In this paper, the moisture storage parameters of three different building materials: ceramic brick, calcium silicate and autoclaved aerated concrete, are measured in the hygroscopic and in the overhygroscopic range.

## 2 Measuring methods

### 2.1 Adsorption and desorption isotherms

The measurements of adsorption isotherms were performed in laboratory conditions, at  $23 \pm 1$  °C. The samples were placed in desiccators with different solutions (see Fig. 1) to simulate different values of relative humidity, see Table 1 [7]. The initial state for all the measurements was dry material. The experiment was performed in parallel in all desiccators in the same way. The mass of samples was mea-



Fig. 1: Desiccator with measured samples

Table 1: Relative humidity over the saturated solutions at  $23 \pm 1$  °C

Salt solution	Relative humidity [%]
LiCl	12
MgCl <sub>2</sub> .6H <sub>2</sub> O	33
NaNO <sub>2</sub>	65
NH <sub>4</sub> Cl	79.5
KNO <sub>3</sub>	94
K <sub>2</sub> Cr <sub>2</sub> O <sub>7</sub>	97

sured in specified time periods until the steady state value of the mass was achieved. Then, the moisture content by volume was calculated according to the equation

$$w = \frac{m_s - m_0}{V \cdot \rho_w} [\text{m}^3/\text{m}^3],$$

where  $m_s$  is the mass of the wet sample in steady state conditions,  $m_0$  is the initial mass of the sample (in dry state),  $V$  is the volume of the sample, and  $\rho_w$  is the density of water at average temperature 20 °C,  $\rho_w = 998 \text{ kg/m}^3$ .

The measurement of desorption isotherms was carried out in the same way as for the adsorption isotherms, except that the initial state was a capillary water saturated specimen.

## 2.2 Moisture retention curves

The experiments were carried out using an ordinary pressure plate device (see Fig. 2). It consists of a compressor inducing pressure above atmospheric pressure, a pressure panel with manometers and regulators, a pressure plate extractor, and ceramic plates (see e.g. [8]).

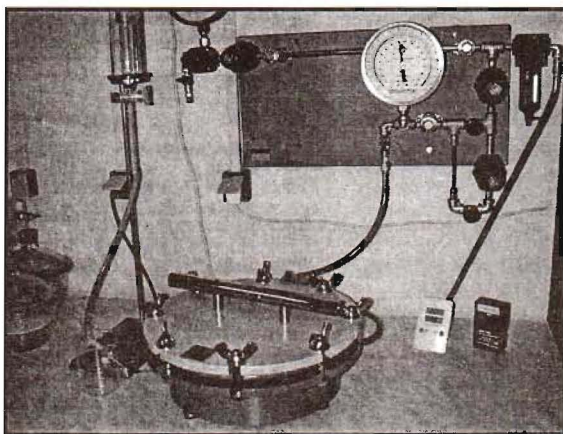


Fig. 2: Experimental setup for moisture retention measurements

The capillary saturated specimens were placed on an air-proof and water saturated ceramic plate covered by a fine kaolin layer and a fine meshed cloth in the pressure plate extractor (see Fig. 3). The extractor was closed, and a chosen pressure was applied. Water drained out of the outflow tube to the outflow burette to achieve equilibrium. When the outflow of water desisted, the extractor was opened, and the mass of the specimens was determined by weighing. The experiment then continued at a new higher-pressure level.

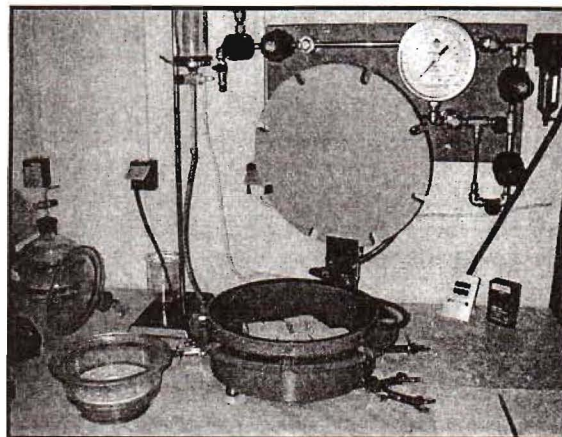


Fig. 3: Placing specimens into the extractor of the pressure plate device

After the measurements were finished the moisture content of the specimen was calculated at each pressure level and a moisture retention curve was constructed.

## 3 Materials and samples

The experiments were carried out on three building materials: calcium silicate plate, ceramic brick and autoclaved aerated concrete (AAC). These materials were chosen because of the differences in pore structure, homogeneity and complexity.

Calcium silicate plate is a low-density board product. In building structures it is mainly used as capillary active inside insulation, because of its very high capillary absorption coefficient and capillary moisture content. It is largely composed of synthetic mineral xonotlite, a complex calcium silicate hydrate (see [9]). Randomly orientated cellulose fibres are also present. Calcium silicate plate has mainly a fine pore structure, comprising the voids between matted acicular crystals. The material can be identified as rather homogeneous and very porous.

Compared to calcium silicate plate, ceramic brick has a tubiform pore structure (see [10]). The total open porosity of the material is much lower. Due to the nature of the material and its production process, higher variability of the material properties can be expected.

The most typical feature of AAC is the presence of artificial air pores created during the production process. The structure of AAC includes spherical air pores. The walls of these pores consist of grains of sand embedded in a cement-lime matrix (see [11]). This matrix provides the cohesion of the material, and consists of fine plate-shaped crystals in a jumble.

In the measurements of adsorption and desorption isotherms, 10 test specimens of each material with overall dimensions of  $30 \times 30 \times 10$  mm; were prepared for each relative humidity.

Experiments to determine the retention curves were carried out with twelve capillary saturated specimens of each material. The size of the specimens was  $35\text{--}40 \times 35\text{--}40 \times 10\text{--}15$  mm<sup>3</sup>. Pressures of 0.16; 0.32; 1.06; 3.16 and 10.0 bar were applied.

## 4 Results and discussion

The results of adsorption and desorption experiments in the hygroscopic range for the particular materials are summarized in Figs. 4–6, where the error ranges of the measurements are also indicated. Calcium silicate was shown to be a very hygroscopic material, and its sorption hysteresis (the difference between the adsorption and desorption isotherms) was quite high. This is in accordance with the presumed fine pore structure of the material. On the other hand, ceramic brick appeared to be an almost non-hygroscopic material. Therefore, its sorption hysteresis is not so important for modeling the material behavior. AAC was found to be somewhere in between the above limits. Its hygroscopicity and also the sorption hysteresis was notable but not so high as in the case of calcium silicate.

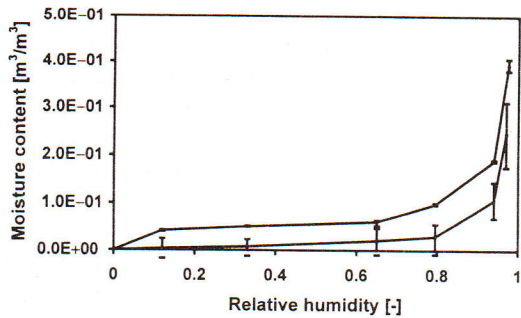


Fig. 4: Adsorption and desorption isotherms of calcium silicate

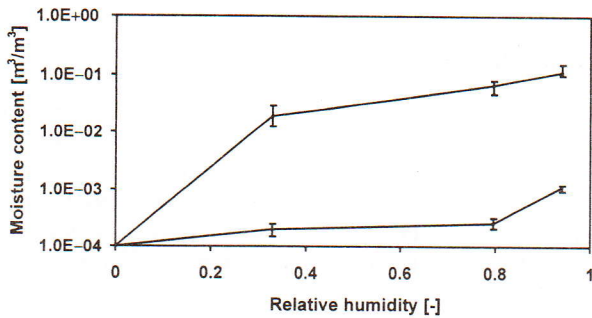


Fig. 5: Adsorption and desorption isotherms of ceramic brick

Figs. 7–9 show the moisture retention curves of the studied materials. The fastest decrease in moisture content with in-

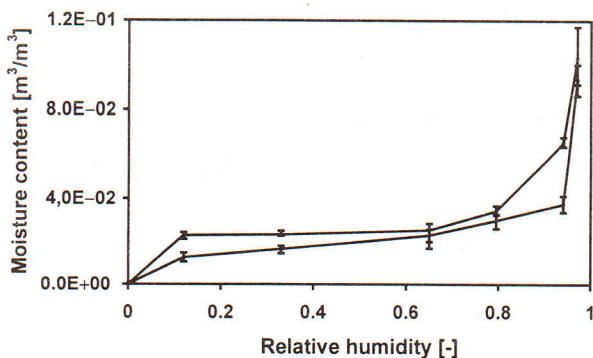


Fig. 6: Adsorption and desorption isotherms of AAC

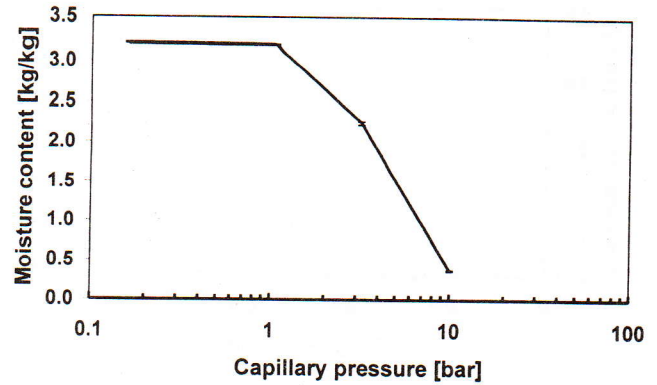


Fig. 7: Moisture retention curve of calcium silicate

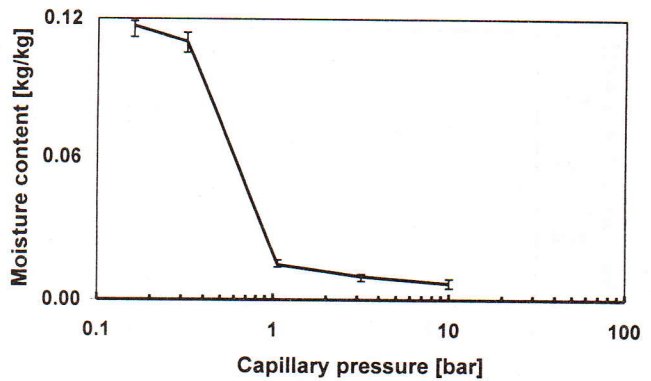


Fig. 8: Moisture retention curve of ceramic brick

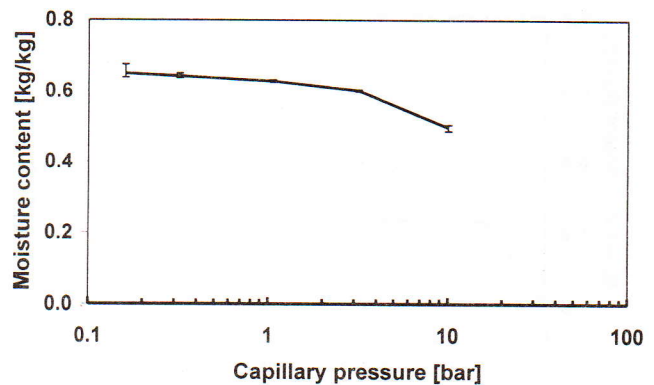


Fig. 9: Moisture retention curve of AAC

creasing pressure was exhibited by ceramic brick, where the characteristic edge on the moisture retention curve appeared at about 0.3 bar. This gives evidence of a substantial amount of large capillary pores. On the other hand, the slowest decrease was observed for AAC, where the edge was found at about 3 bar. This indicates that the relative amount of capillary pores in this material should be lowest among the studied materials. The results obtained for calcium silicate were in between. The edge on the moisture retention curve appeared at about 1 bar.

Figs. 10–12 present the moisture storage functions constructed from the desorption isotherms and moisture retention curves using recalculation of capillary pressure to relative humidity by the Kelvin equation. Clearly, the hygro-

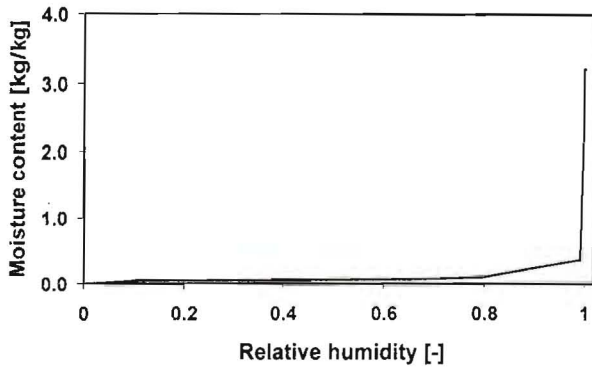


Fig. 10: Moisture storage function of calcium silicate

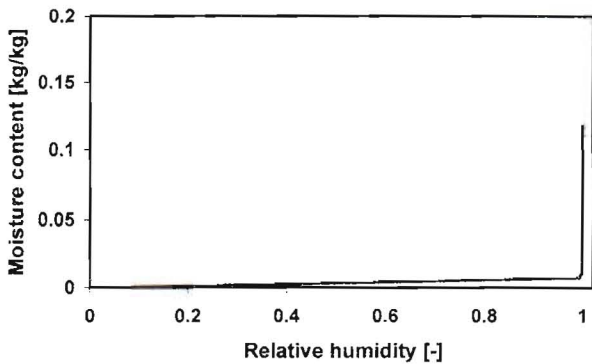


Fig. 11: Moisture storage function of ceramic brick

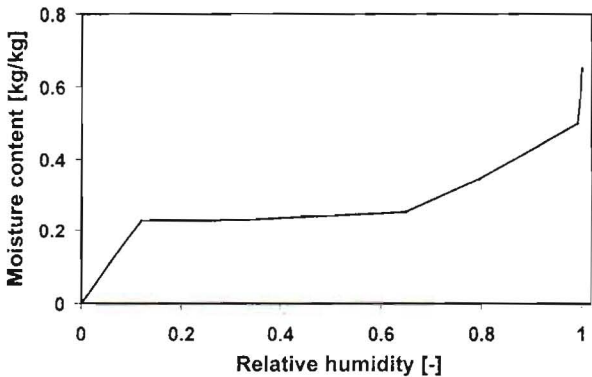


Fig. 12: Moisture storage function of AAC

scopic and overhygroscopic parts of the curves are monotonic. They correspond for all materials, and no ambiguities appear.

The results of the moisture retention measurements should approximately agree with the porosimetric measurements, as already indicated in the explanation of the shape of the curves. Therefore, additional mercury porosimetry measurements were carried out to verify this agreement. In these experiments, a Micromeritics PORESIZER 9310 mercury intrusion porosimeter with a maximum working pressure of 200 MPa and pore distribution in the range 300  $\mu\text{m}$  to 0.006  $\mu\text{m}$  was employed.

It is well known that the results of mercury intrusion porosimetry have to be interpreted with care, particularly

the distribution curves, which can be negatively affected for instance by the presence of necks of larger pores (see, e.g., [12] for details). We therefore present only global characteristics of the pore space of the particular materials. Table 2 gives the total intrusion volume  $V_p$ , the total pore area  $A_p$ , and the median pore radius by volume  $r_v$ .

Table 2 Global characteristics of the pore space

Material	$V_p$ [cm <sup>3</sup> /g]	$A_p$ [m <sup>2</sup> /g]	$r_v$ [mm]	$r_{\text{steep}}$ [mm]
Calcium silicate	3.22	75.00	0.27	0.14–1.44
Ceramic brick	0.10	3.12	2.70	1.44–4.80
AAC	0.90	67.85	0.084	?–0.48

In order to compare the moisture retention data with the mercury porosimetry data, the capillary pressures corresponding to the beginning and end of the steep parts of the moisture retention curves were recalculated to the respective pore radii. The results are shown in Table 2 in column  $r_{\text{steep}}$ , where the first number corresponds to the end and the second number corresponds to the beginning of the steep part of the particular moisture retention curve. Clearly, the median pore radii determined by mercury intrusion porosimetry fall within the limits given by these two values, so that the agreement between the two methods can be considered as satisfactorily.

## 5 Conclusions

Solution of the increasingly complex problems of moisture transport in building materials requires the application of advanced computer codes involving simultaneous utilization of both liquid water and water vapor related storage properties. However, in many building-physics laboratories only the hygroscopic parts of moisture storage functions – the sorption isotherms – are commonly measured. In this paper, the moisture storage functions of three different building materials were determined in the whole moisture range. The parts of the curves corresponding to the hygroscopic and overhygroscopic ranges correspondent together, and the curves were also in good agreement with other basic requirements for this type of function. A comparison of the liquid water related parts of the moisture storage functions with the results of mercury intrusion porosimetry exhibited reasonable agreement for all three materials.

## Acknowledgements

This research has been supported by the Ministry of Education of the Czech Republic, under contract No. MSM:210000003.

## References

- [1] Černý, R., Rovnaníková, P.: *Transport Processes in Concrete*. London: Spon Press, 2002.

- [2] Hansen, K. K.: *Sorption Isotherms*. Technical Report 163/86. Lyngby: Technical University of Denmark, 1986.
- [3] Brocken, H. J. P.: *Moisture Transport in Brick Masonry: the Grey Area Between Bricks*. PhD Thesis, Eindhoven: TU Eindhoven, 1998.
- [4] Roels, S.: *Modeling Unsaturated Moisture Transport in Heterogeneous Limestone*. PhD Thesis, Leuven: Katholieke Universiteit Leuven, 2000.
- [5] Hillel, D.: *Fundamentals of Soil Physics*. New York: Academic Press, 1980.
- [6] Grunewald, J.: *DELPHIN 4.1 – Documentation*. Theoretical Fundamentals. Dresden: TU Dresden, 2000.
- [7] Arai, C., Hosaka, S., Murase, K., Sano, Y.: *Measurements of the Relative Humidity of Saturated Aqueous Salt Solutions*, J. Chem. Eng. Jap., Vol. 9, 1976, p. 328–330.
- [8] SBI Report 295: *Retention Curves Measured Using Pressure Plate and Pressure Membrane Apparatus*. Horsholm: Danish Building Research Institute, 1998.
- [9] Hamilton, A., Hall, C.: *Composition and Additional Characterisation of Calcium Silicate Material: Revision with new Data*. 5<sup>th</sup> Framework EU HAMSTAD – project, working document, Edinburgh: University of Edinburgh, 2003.
- [10] Carmeliet, J., Descamps, F., Houvenaghel, G.: *A Multi-scale Network Model for Simulating Moisture Transfer Properties of Porous Media*. Transport in Porous Media, Vol. 35, 1999, p. 67–88.
- [11] Roels, S., Sermijn, J., Carmeliet, J.: *Modelling Unsaturated Moisture Transport in Autoclaved Aerated Concrete: a Micro-structural Approach*. In: Building Physics in the Nordic Countries. Proceedings of the 6<sup>th</sup> symposium, Trondheim, June 17–19, 2002. Eds. Gustavsen A. and Thue J. V., Trondheim: Norwegian Building Research Institute and Norwegian University of Science and Technology, 2002.
- [12] Diamond, S.: *Mercury Porosimetry: An Inappropriate Method for the Measurement of Pore Size Distributions in Cement-based Materials*. Cement and Concrete Research, Vol. 30, 2000, p. 1517–1525.

---

Ing. Milena Jiříčková  
phone: +420 224 354 498  
e-mail: jiricko@fsv.cvut.cz

Prof. Ing. Robert Černý, DrSc.  
phone: +420 224 354 429  
e-mail: cernyr@fsv.cvut.cz

Department of Structural Mechanics

Czech Technical University in Prague  
Faculty of Civil Engineering  
Thákurova 7  
166 29 Prague 6, Czech Republic

Doc. RNDr. Pavla Rovnaníková, CSc.  
phone: +420 541 147 633  
e-mail: chrov@fce.vutbr.cz

Institute of Chemistry  
Faculty of Civil Engineering  
Technical University of Brno  
Žižkova 17  
662 37 Brno, Czech Republic